This is the peer reviewed version of the following article: Gracia R, Marradi M, Cossío U, et al. Synthesis and functionalization of dextran-based single-chain nanoparticles in aqueous media. J Mater Chem B. 2017;5(6):1143-1147, which has been published in final form at doi: 10.1039/C6TB02773C. This article may be used for non-commercial purposes in accordance with Royal Society of Chemistry Terms and Conditions for Self-Archiving.

Synthesis and Functionalization of Dextran–Based Single–Chain Nanoparticles in Aqueous Media

R. Gracia,[a] M. Marradi,[a] U. Cossío,[b] A. Benito,[a] A. Pérez-San Vicente,[a] V. Gómez-Vallejo,[b] H.-J. Grande,[a] J. Llop[b] and I. Loinaz[a,*]

[a.] *Biomaterials Unit, IK4-CIDETEC, Pº Miramón 196, 20014, Donostia-San Sebastián, Spain.*
[b.] *Radiochemistry and Nuclear Imaging Group, CIC biomaGUNE, Pº Miramón 182, 20014, Donostia-San Sebastián, Spain.*

Water-dispersible dextran-based single-chain polymer nanoparticles (SCPNs) were prepared in aqueous media and mild conditions. Radiolabeling of the resulting biocompatible materials allowed the study of lung deposition of aqueous aerosols after intratracheal nebulization by means of single-photon emission computed tomography (SPECT), demostrating their potential use as imaging contrast agents.

Advances in engineering polymer chains at the molecular level[1] have pushed the development of synthetic strategies for the controlled compaction of single polymer coils into unimolecular soft nano-objects, named single-chain polymer nanoparticles (SCPNs).[2-4] SCPNs based on synthetic polymers benefit from the possibility of a controlled construction of the precursors in order to prepare tuned SCPNs with desired size and functionality.[3] Additionally, a wide variety of biocompatible, non-toxic and ready-to-use natural polymers are available. Consequently, SCPNs have gained interest as potential mimetics of biomacromolecules such as proteins[5,6]
and for application in different fields including nanomedicine.[7-9] Among natural polymers, polysaccharides can be envisaged as natural analogues of polyethylene glycol (PEG). For example, dextrans have been used in several biomedical applications due to aqueous solubility, biocompatibility, biodegradability, wide availability, ease of modification and non-fouling properties.[10,11] However, *in vivo* application of SCPNs can be limited due to their small size. Rapid blood clearance is expected after intravenous administration of particles below 5 nm size.[12] In the last years, non-invasive lung administration route has been broadly studied,[13] and SCPNs could be beneficial due to their small size.[14]

Synthetic routes to SCPNs are mainly based on intrachain homo- and hetero-coupling or cross-linking-induced collapseof pre-functionalized polymers through covalent, dynamic covalent, and non-covalent bonding.[15,16] Most of the covalent strategies are performed in organic solvents and require highly diluted polymer solutions (usually <1 mg/mL), high temperatures and/or the presence of metal catalysts. The preparation of SCPNs through "continuous addition" avoids ultra-dilution conditions, which is beneficial for multigram scale preparations.[17] Recently, it has been described that the presence of oligo(ethylene glycol) brushes as side-chains allows to achieve SCPNs at high polymer concentrations (100 mg/mL).[18] However, the development of general procedures to obtain functionalizable SCPNs in aqueous media, mild conditions and scalable conditions is still a challenging issue.

Our group reported a strategy to generate structurally defined and water-dispersible poly(methacrylic acid)-based SCPNs.[19] In pursuit of novel types of biocompatible polymeric nanoparticles based on readily available and easily functionalized materials, we here present a novel and straightforward synthetic methodology to obtain small (approximately 13 nm) dextran (DXT)-based SCPNs through the intramolecular crosslinking (compaction) of single polysaccharide chains by means of a homobifunctional crosslinker in aqueous media and mild conditions. Dextran-40 (40 KDa, **DXT**) and 3,6-dioxa-1,8-octane-dithiol (**DODT**), both commercially available and relatively cheap, were selected as the polysaccharide and the cross-linker, respectively. Chemical modification of **DXT** following an established protocol[20] with minor modifications led to the formation of the dextranmethacrylate derivative (**DXT-MA**) which could react with **DODT** through thiol-ene Michael addition (covalent approach) at room temperature, air atmosphere, and in absence of any catalysts (Scheme 1). Thiol-based Michael additions[21] have recently gained importance in polymer and materials synthesis.[22] Using highly polar solvents such as water and under controlled pH, thiols can be used as Michael donors in additions which proceed with high yields and selectivity in mild and clean conditions.[23-25] SCPNs resembling disordered proteins were recently prepared by Pomposo *et al.* through classic Michael addition between polymeric precursors

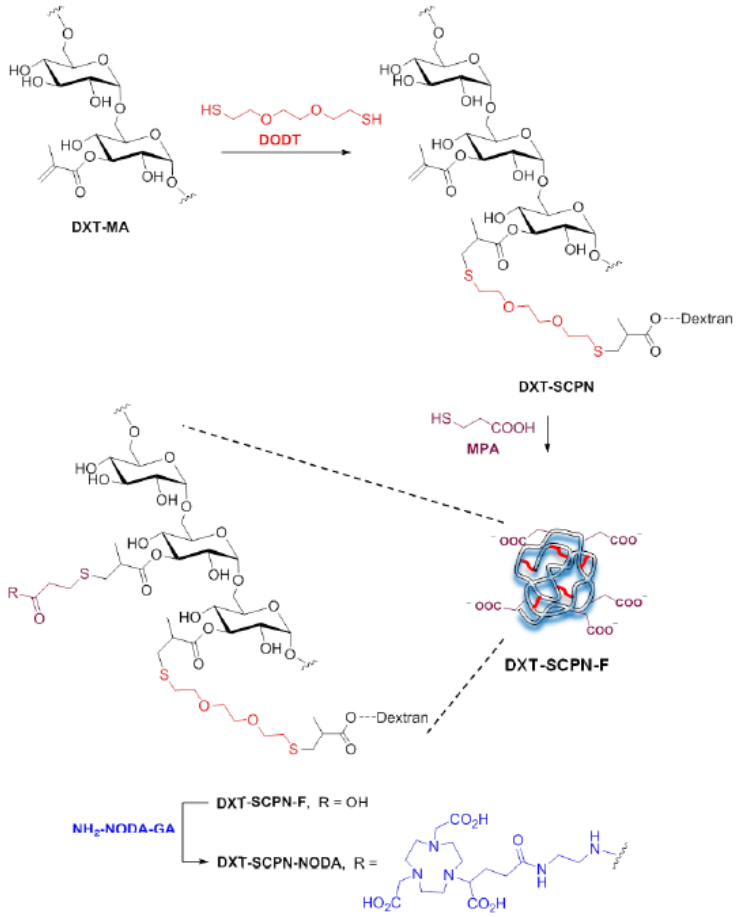

Scheme 1. Synthesis and functionalization of dextran-based single-chain nanoparticles.

containing β-ketoester groups (Michael donors) and external acrylate-based cross-linkers (Michael acceptors) under highdilution conditions in organic solvent.[26]

The degree of substitution of **DXT-MA** (DS, MA groups per repeating unit) was around 52%, which is high enough to allow for both intrachain collapse and further functionalization of **DXT-SCPN** and low enough to maintain water dispersibility. As an example of functionalization, we incorporated carboxylic groups into **DXT-SCPN** by reaction with mercaptopropionic acid (**MPA**). This, in turn, enabled the incorporation of the commercially available chelating agent 2,2'-(7-(4-((2- aminoethyl)amino)-1-carboxy-4-oxobutyl)-1,4,7-triazonane- 1,4-diyl) diacetic acid (**NH2-NODA-GA**) *via* amidic coupling. The NODA macrocycle was used to chelate the radionuclide Gallium-67 (^{67}Ga), suitable for subsequent *in vivo* imaging using single photon emission computerized tomography (SPECT). As a proof of concept of potential applications of the labeled SCPNs, we investigated the regional lung deposition of aqueous aerosols after intratracheal nebulization.

The formation of **DXT-SCPN** was achieved by continuous addition of a 0.16M solution of cross-linker **DODT** to a relatively concentrated dispersion (1 wt%, i.e. 10 mg/mL) of the precursor **DXT-MA** in PBS at room temperature and air atmosphere. The preparation of intra- and intermolecular cross-linked dextran *via* free radical polymerization in ultradilute conditions under a nitrogen atmosphere has been previously reported by Hennink.[27] In our case, the pH was adjusted at 9-9.5 for the reaction to take place smoothly in the presence of nucleophilic thiolates. Higher pH values were detrimental due to an increased level of ester hydrolysis. The reaction conditions were adjusted to maintain the formation of SCPNs and to prevent intercross-linking. Slow controlled addition (0.04 mL/h) of **DODT** (0.5 equivalents in terms of thiols respect to the MA present in the polysaccharide backbone) to the dispersion of **DXT-MA**, that circumvent ultradilution of the polymer,[17] afforded the desired **DXT-SCPN**. The absence of non-reacted thiol groups from the cross-linker was verified by reassessed Elmann's test.[28]

Upon intramolecular cross-linking of precursor **DXT-MA**, a reduction of the intensity of the signals corresponding to the MA protons was observed by ^{1}H NMR (signals c, Fig. 1), while new signals due to **DODT** (b′, c′, d) appeared at

around 2.6-3.0 ppm in the spectrum of **DXT-SCPN**. The intensity of methyl signal at 1.98 ppm (signal a) in the precursor **DXT-MA** decreased in favor of its correspondent signal at 1.29 ppm, i.e. the methyl in beta position with respect to the sulfur atom of the cross-linker (signal a′). The conversion of Michael addition was quantitative and around half of initial methacrylate groups remained available for further functionalization.

The functionalization of polymer nanoparticles is object of intense research.[23,29] In order to enable further functionalization of **DXT-SCPN**, thiol-ene Michael addition of **MPA** was carried out. Complete disappearance of the MA protons (signals c, Fig. 1) and the methyl signal at 1.98 ppm (signal a) in the ^{1}H NMR spectrum indicated that the reaction proceeded successfully. The methyl group completely shifted below 1.30 ppm (a′ and a″) and the MPA appeared at 2.4-3.0 ppm (h and g). The incorporation of **MPA** was also confirmed by Z-potential measurements (Fig. S6) with a decrease from the neutral surface charge of the **DXT-MA** to negative values for **DXT-SCPN-F** (around -20 mV) due to the presence of the carboxylate groups. Furthermore, the overall process was also performed by sequentially adding **DODT** and **MPA** without isolation/purification of the **DXT-SCPN** intermediate.

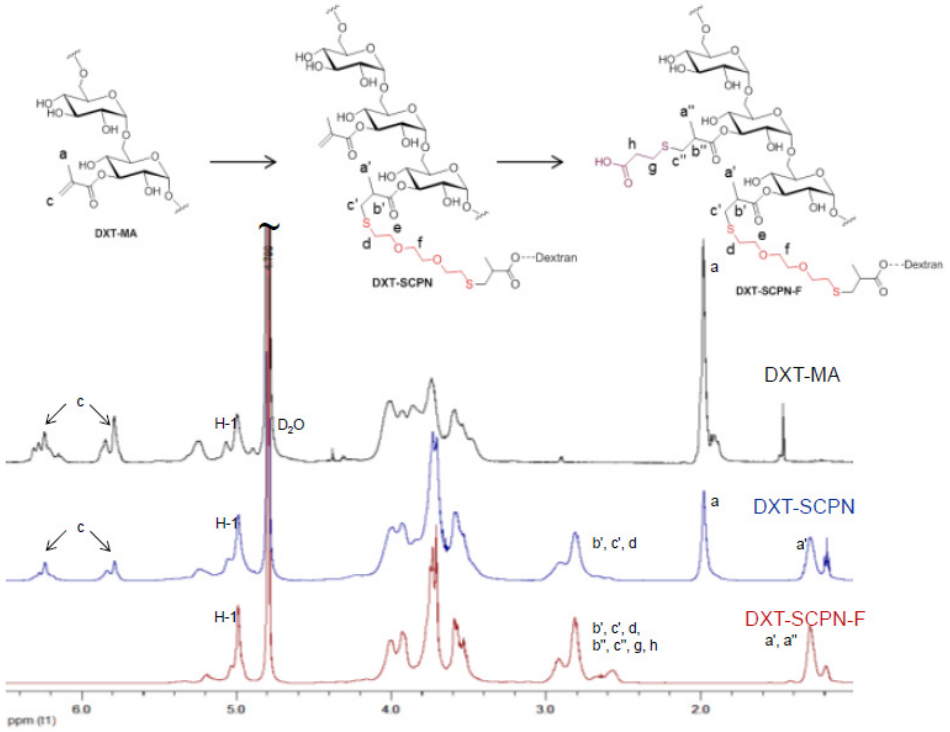

Figure 1. ^{1}H NMR spectra (D_2O, 500 MHz) of **DXT-MA** (top), **DXT-SCPN** (middle), and **DXT-SCPN-F** (bottom).

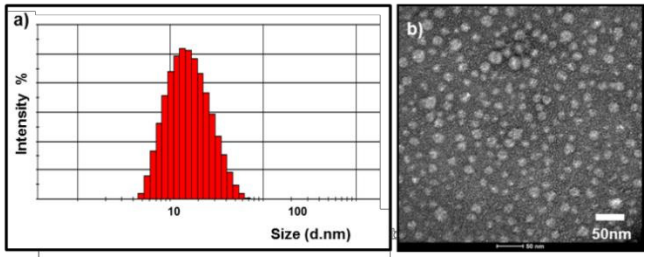

Figure 2. (a) DLS of **DXT-SCPN-F** and (b) TEM micrograph.

Transmission electron microscopy (TEM) and DLS were performed to get insights about the size and shape of the nanoparticles (Fig. 2). TEM micrographs were obtained after uranyl staining. In the dry state, **DXT-SCPN-F** adopt a compact, globular morphology with an average diameter of 13±3 nm (Fig. 2b). Hydrodynamic diameter (D_h), measured by DLS in saline (0.9 wt% NaCl), revealed a Z-average of 15±4 nm for **DXT-SCPN-F** (Fig. 2a). No significant difference with respect to the non-functionalized **DXT-SCPN** was found (Fig. S2). The formation of non-uniform nanoparticles (high polydispersity index) is related to the broad molecular weight distribution of the branched precursor polymer.

For GPC experiments, a control system (**DXT-MA-F**, Fig. S8) was prepared by treating the starting precursor with **MPA** in order to compare macromolecules with similar molecular weight (*Mw*) and polarity. The increase of retention time in **DXT-SCPN-F** with respect to **DXT-MA-F**, in spite of the similar *Mw*, is in agreement with a reduction of the hydrodynamic radius and gives evidence for single-chain compaction (Fig. 3).

^{1}H detected diffusion ordered spectroscopy (DOSY) has been also used to get deeper insights of the compaction effect due to the intracross-linking process.[30] DOSY experiments were carried out to determine the diffusion coefficient (*D*) of the different species in solution. *D* is inversely proportional to the hydrodynamic radius so that the intramolecular compaction should produce an increase of this parameter at

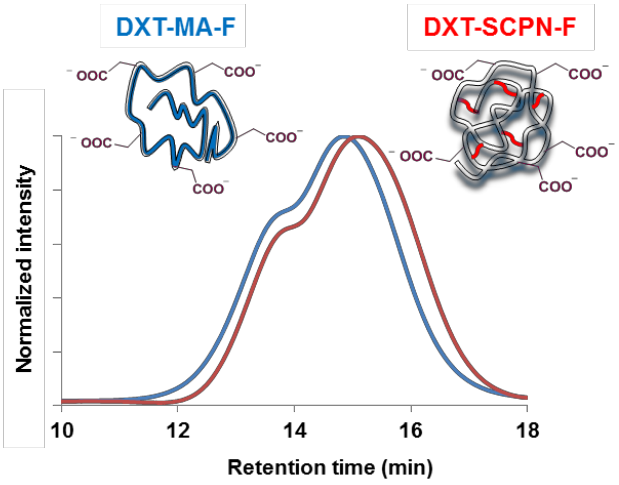

Figure 3. GPC chromatograms of control dextran polymer **DXT-MA-F** (blue) and **DXT- SCPN-F** (red).

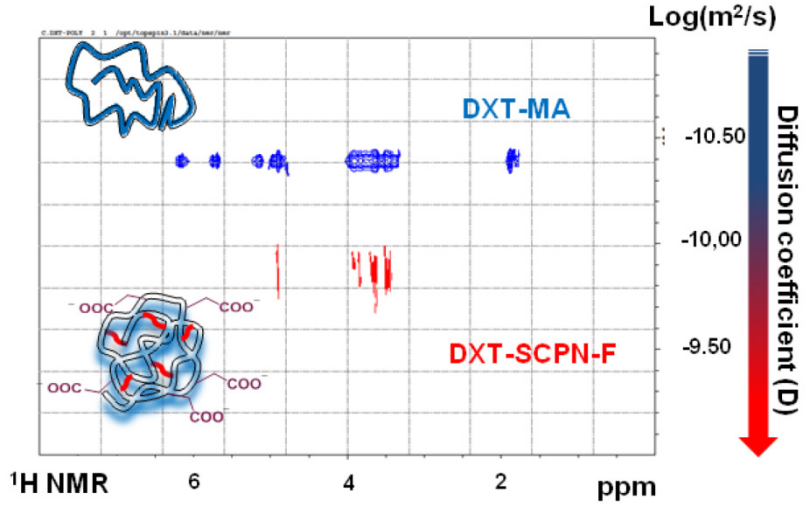

Figure 4. DOSY spectra of **DXT-SCPN-F** (red) and **DXT-MA** (blue).

equal concentration and dynamic viscosity values (Stokes- Einstein equation). The diffusion coefficient values for **DXT-MA** and **DXT-SCPN** (10 mg/mL in D2O) were 40.7 and 135 μm2/s (in Fig. 4, -10.39 and -9.87 log(m2/s)) respectively, indicating a different behavior of the two macromolecules in solution.

It is known that the collapse from polymers to the corresponding SCPNs produces a significant drop in viscosity,[31] thus we decided to perform *D* measurements in dilute conditions (1 mg/mL in D2O).[32] Measurements of the time evolved concentration profile (Taylor Dispersion Analysis) on the basis of Ultraviolet (UV) absorbance plotted as a function of time, were performed to determine the molecular diffusion coefficient using Viscosizer TD (Malvern). Diffusion coefficients of 56.8 μm2/s and 383.3 μm2/s were obtained for the precursor **DXT-MA** and **DXT-SCPN-F**, respectively. This increase indicates a lower resistance to flow of **DXT-SCPN** with respect to the starting **DXT-MA** polymer and constitutes a direct proof of compaction..

After purification by dialysis, **DXT-SCPN-F** could be freezedried and redispersed in water. ^{1}H NMR stability controls at pH 7.4 demonstrated that no significant hydrolysis takes place during at least 2 months (data not shown). No cytotoxicity was found in HeLa cells up to 50 µg/mL (Fig. S9).

In order to show potential applications of the nanoparticles developed here, the chelating agent NODA was anchored by covalent chemistry through DMTMM-mediated amidic coupling between the amino group of **NH2-NODA-GA** and the carboxyl group of **DXT-SCPN-F** (Scheme 1). NODA is suitable to chelate radiometals such as the gamma emitter ^{67}Ga, which enables subsequent SPECT imaging. ^{67}Ga was selected as the radioisotope because of its appropriate gamma emission properties and long half-life, which may enable longitudinal follow-up of the radioactive signal over days, if required. Radiolabeling of **DXT-SCPN-NODA** was based on the formation of the chelator-radiometal complex. Previous works showed that this strategy is perfectly suited for the preparation of ^{67}Ga-labeled nanoparticles.[33] At pH 4.2, reaction time 45 min, and reaction temperature 25 °C, radiochemical yields of 51 ± 5% (non decay corrected) were achieved. Stability studies in acetate buffer solution showed that >95% of the radioactivity was still attached to the nanoparticles at t=48 h of incubation, and the percentage of released ^{67}Ga was <10% at t=144 h.

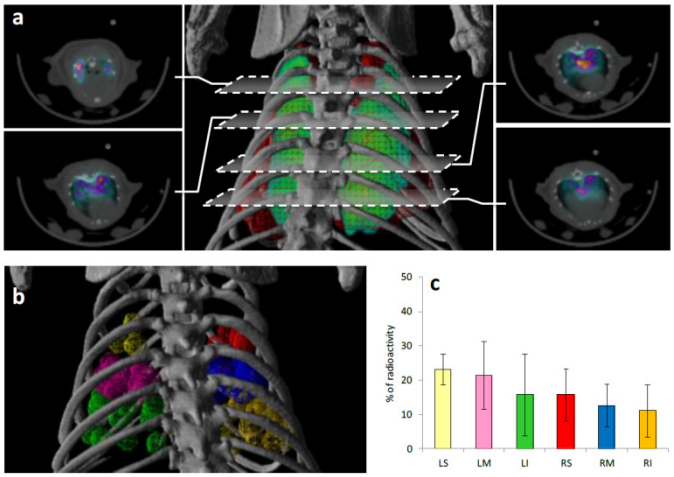

Figure 5. (a) SPECT-CT images obtained after administration of ^{67}Ga-labeled SCPNs by intratracheal nebulization; 3D CT images of the skeleton(grey)/lungs (red) co-registered with volume-rendered 3D SPECT images (green tones) are shown (middle), together with representative axial SPECT-CT slices of the thoracic cavity (left and right); (b) VOIs drawn in the different regions of the lungs; (c) Percentage of radioactivity in each region; LS: Left superior; LM: left medium; LI: left inferior; RS: right superior; RM: right medium; RI: right inferior.

The labeled particles were used to assess the regional lung distribution of an aqueous aerosol generated with the Penn- Century MicroSprayer® aerosolizer. The regional lung distribution in rodents using this aerosolizer has been already investigated using *in vivo* optical imaging.[34] However, this imaging technique has certain limitations in terms of image quantification and translation into large species or humans, due to the low penetration capacity of visible and infrared light. The SPECT-CT images acquired immediately after administration of the labeled SCPN confirmed the presence of nanoparticles over the whole lungs, although the regional distribution was not completely homogeneous (Fig. 5a). Importantly, the delineation of volumes of interest (VOIs, Fig. 5b) and further quantification resulted in quantitative data regarding regional lung distribution (Fig. 5c). The results clearly show that certain regions of the lungs are underexposed.
Altogether, these results suggest that the administration protocol is appropriate for nebulization of aerosols in rat lung, although sub-optimal results might be obtained when a uniform distribution of the administered aerosol is paramount.

Conclusions

In summary, a straightforward way to biocompatible and easy to handle dextran-based single-chain nanoparticles has been described. Incorporation of chemical reactive groups such as carboxylic acids on the surface of the nanoparticles offers the possibility to conjugate (bio)molecules to the nanoparticles. As a proof of principle, a NODA derivative was incorporated, the SCPNs were radiolabeled with ^{67}Ga and the labelled particles were used to assess regional lung deposition of an aqueous aerosol in rats. By incorporation of further functionalities, it is anticipated that these SCPNs may find use as contrast agents for diagnosis of pulmonary diseases.

Acknowledgements

This project has received funding from the European Union's Seventh Framework Programme for research, technological development and demonstration under grant agreement no 604434 (PneumoNP). This research was also supported by the Departamento de Desarrollo Económico y Competitividad of the Basque Government, under the Elkartek 2015 program, project biomagune 2015, ref. KK- 2015/0000088, and by the Spanish Ministry of Economy and Competitiveness, project MAT2013-48169-R. We thank Idoia Tolosa for technical support. Samir Safi (Malvern Instruments Ltd) and Mariano Barrado (UPV-EHU) are acknowledged for helpful assistance with Viscosizer TD and TEM, respectively.Competitiveness, project MAT2013-48169-R. We thank Idoia Tolosa for technical support. Samir Safi (Malvern Instruments Ltd) and Mariano Barrado (UPV-EHU) are acknowledged for helpful assistance with Viscosizer TD and TEM, respectively.

Notes and references

1 M. Ouchi, N. Badi, J.-F. Lutz and M. Sawamoto Nat. Chem. 2011, 3, 917–924.
2 M. K. Aiertza, I. Odriozola, G. Cabañero, H.-J. Grande and I. Loinaz Cell. Mol. Life Sci. 2012, 69, 337–346.
3 A. M. Hanlon, C. K. Lyon and E. B. Berda Macromolecules 2016, 49, 2–14.
4 M. Gonzalez-Burgos, A. Latorre-Sanchez and J. A. Pomposo Chem. Soc. Rev. 2015, 44, 6122–6142.
5 M. Huo, N. Wang, T. Fang, M. Sun, Y. Wei and J. Yuan Polymer 2015, 66, A11–A21.
6 O. Altintas and C. Barner-Kowollik Macromol. Rapid Commun. 2016, 37, 29−46.
7 S. K. Hamilton and E. Harth ACS Nano 2009, 3, 402–410; C.-C. Cheng, D.-J. Lee, Z.-S. Liao and J.-J. Huang Polym. Chem., 2016,7, 6164-6169; I. Perez-Baena, I. Loinaz, D. Padro, I. García, H. J. Grande and I. Odriozola J. Mater. Chem. 2010, 20, 6916-6922.
8 D. E. Whitaker, C. S. Mahon and D. A. Fulton Angew. Chem. Int. Ed. 2013, 52, 956–959.
9 I. Odriozola, M. K. Aiertza, G. Cabañero, H.-J. Grande and I. Loinaz, in Handbook of Harnessing Biomaterials in Nanomedicine: Preparation, Toxicity, ed. Dan Peers, CRC Press, Taylor & Francis Group, Boca Raton (FL), 2012, chapter 2, 21–42.
10 M. Naessens, A. Cerdobbel, W. Soetaert and E. J. Vandamme Chem. Technol. Biotechnol. 2005, 80, 845–860.
11 S. R. Van Tomme and W. E. Hennink Expert Rev. Med. Devices 2007, 4, 147–164.
12 M. Longmire, P. L. Choyke and H. Kobayashi Nanomedicine 2008, 3, 703–717.
13 P. Colombo, F. Sonvico and F. Buttini, in Nanostructured Biomaterials for Overcoming Biological Barriers, ed. Maria Jose Alonso and Noemi S. Csaba; RSC Drug Discovery Series No. 22; The Royal Society of Chemistry, Cambridge (UK), 2012, chapter 5.2, 273–299.
14 X. Murgia, P. Pawelzyk, U. F. Schaefer, C. Wagner, N. Willenbacher and C.-M. Lehr Biomacromolecules 2016, 17, 1536−1542.
15 C. K. Lyon, A. Prasher, A. M. Hanlon, B. T. Tuten, C. A. Tooley, P. G. Franka and E. B. Berda Polym. Chem. 2015, 6, 181–197.
16 M. Artar, E. Huerta, E. W. Meijer and A. R. A. Palmans, in Sequence-Controlled Polymers: Synthesis, Self-Assembly, and Properties; ed. Jean-François Lutz, Tara Y. Meyer, Makoto Ouchi, Mitsuo Sawamoto; ACS Symposium Series; American Chemical Society, Washington, DC, 2014, vol. 1170, chapter 21, 313–325.
17 E. Harth, B. Van Horn, V. Y. Lee, D. S. Germack, C. P. Gonzales, R. D. Miller and C. J. Hawker *J. Am. Chem. Soc.* 2002, **124**, 8653–8660.
18 E. H. H. Wong, S. J. Lam, E. Nam and G. G. Qiao *ACS Macro Lett.* 2014, **3**, 524−528.
19 A. B. Benito, M. K. Aiertza, M. Marradi, L. Gil-Iceta, T. Shekther Zahavi, B. Szczupak, M. Jiménez-González, T. Reese, E. Scanziani, L. Passoni, M. Matteoli, M. De Maglie, A. Orenstein, M. Oron-Herman, G. Kostenich, L. Buzhansky, E. Gazit, H.-J. Grande, V. Gómez-Vallejo, J. Llop and I. Loinaz *Biomacromolecules* 2016, *DOI: 10.1021/acs.biomac.6b00941*
20 W. N. E. van Dijk-Wolthuis, J. J. Kettenes-van den Bosch, A. van der Kerk-van Hoof and W. E. Hennink *Macromolecules* 1997, **30**, 3411−3413.
21 B. D. Mather, K. Viswanathan, K. M. Miller and T. E. Long *Prog. Polym. Sci*. 2006, **31**, 487–531.
22 C. E. Hoyle, A. B. Lowe and C. N. Bowman *Chem. Soc. Rev.* 2010, **39**, 1355–1387.
23 H. Kakwere and S. Perrier *J. Am. Chem. Soc*. 2009, **131**, 1889– 1895.
24 G.-Z. Li, R. K. Randev, A. H. Soeriyadi, G. Rees, C. Boyer, Z. Tong, T. P. Davis, C. Remzi Becera and D. M. Haddleton *Polym. Chem.* 2010, **1**, 1196–1204.
25 Q. Tang, B. Cao, X. Lei, B. Sun, Y. Zhang and G. Cheng *Langmuir* 2014, **30**, 5202–5208.
26 A. Sanchez-Sanchez, S. Akbari, A. Etxeberria, A. Arbe, U. Gasser, A. J. Moreno, J. Colmenero and J. A. Pomposo *ACS Macro Lett*. 2013, **2**, 491–495.
27 O. Franssen, R. D. van Ooijen, D. de Boer, R. A. A. Maes and W. E. Hennink *Macromolecules* 1999, **32**, 2896-2902.
28 P. W. Riddles, R.L.Blakeley, B. Zerner Meth. Enzymol. 1983, 91, 49–60.
29 B. Korthals, M. C. Morant-Miñana, M. Schmid and S. Mecking *Macromolecules* 2010, **43**, 8071–8078.
30 N. Ormategui, I. García, D. Padro, G. Cabañero, H. J. Grande and I. Loinaz *Soft Matter* 2012, **8**, 734–740.
31 J. B. Beck, K. L. Killops, T. Kang, K. Sivanandan, A. Bayles, M.E. Mackay, K. L. Wooley and C. J. Hawker *Macromolecules*2009, **42**, 5629–5635.
32 N. H. Maina, L. Pitkänena, S. Heikkinen, P. Tuomainen, L.Virkki and M. Tenkanen, *Carbohydr. Polym.* 2014, **99**, 199–207.

33 D. W. Hwang, H. Y. Ko, J. H. Lee, H. Kang, S. H. Ryu, I. C. Song, D. S. Lee, S. Kim, *J. Nucl. Med.* 2010, **51**, 98–105.
34 C. Duret, N. Wauthoz, R. Merlos, J. Goole, C. Maris, I. Roland, T. Sebti, F. Vanderbist and K. Amighi *Eur. J. Pharm. Biopharm.* 2012, **81**, 627–634.

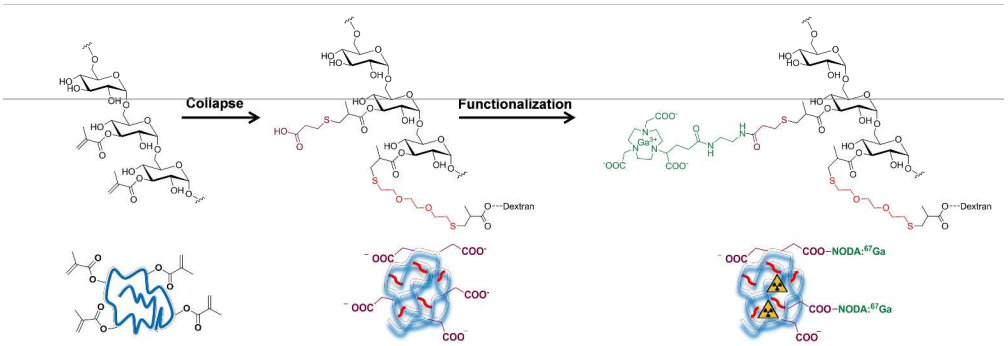

1587x599mm (96 x 96 DPI)

SUPPORTING INFORMATION
Synthesis and Functionalization of Dextran–Based Single–Chain Nanoparticles in Aqueous Media

Raquel Gracia,a Marco Marradi,a Unai Cossío,b Ana Benito,a Adrián Pérez-San Vicente,a Vanessa Gómez-Vallejo,b Hans-Jürgen Grande,a Jordi Llop,b Iraida Loinaza,* aBiomaterials Unit, IK4-CIDETEC, Pº Miramón 196, 20014, Donostia-San Sebastián, Spain; bRadiochemistry and Nuclear Imaging Group, CIC biomaGUNE, Pº Miramón 182, 20014, Donostia-San Sebastián, Spain.

Materials and methods

Dextran from *Leuconostoc* spp. (DXT-40, Mr ~40 kDa), glycidyl methacrylate (GMA) (97%), dimethyl sulfoxide (DMSO) (98%), 3-mercaptopropionic acid (≥99%), 4-(4,6- dimethoxy-1,3,5-triazin-2-yl)-4-methylmorpholinium chloride (DMTMM·HCl) (96%) and 2,2′-(ethylenedioxy)diethanethiol [3,6-dioxa-1,8-octane-dithiol (**DODT**)] (95%) were purchased from Aldrich. Phosphate-buffered saline (PBS) was purchased from Scharlau. 4-(Dimethylamino)pyridine (DMAP) was purchased from Acros-Organics. 2,2'-(7-(4-((2-Aminoethyl)amino)-1-carboxy-4-oxobutyl)-1,4,7-triazonane-1,4- diyl)diaceticacid (**NH2-NODA-GA**) (98%) was purchased from CheMatech. Water (H2O) used in the syntheses, unless otherwise stated, was deionized water from a MilliQ A10 Gradient equipment (Millipore).

Dynamic Light Scattering (DLS): DLS analyses were conducted using a Zetasizer Nano ZS, ZEN3600 Model (Malvern Instruments Ltd). All measurements were performed in disposable sizing cuvettes at a laser wavelength of 633 nm and a scattering angle of 173°, while the zeta-potential measurements were performed in disposable zeta potential cells (pH 7.4, 25 ºC). Before the measurement, the samples were dispersed in saline solution (0.9 wt% NaCl for size measurements and 1 mM NaCl for zeta-potential measurements) at a concentration of 1 mg/mL. Each measurement was repeated for three runs per sample at 25 °C.

Gel permeation chromatography (GPC): The weight-average molecular weight (*Mw*), number-average molecular weight (*Mn*) and polydispersity index (PDI; *Mw/Mn*) were measured at 40 ºC on an Agilent GPC-50 system equipped with 2x PL-Aquagel Mixed- OH, Guard-Aquagel-OH columns and a differential refractive index (RI) detector. 0.3 M NaNO3, 0.01 M NaH2PO4, pH 7 was used as eluent at a flow rate of 1 mL/min. The system was calibrated using polyethylene oxide (PEO) standards.

Transmission electron microscopy (TEM): TEM analyses were performed in a TECNAI G2 20 TWIN microscope (FEI, Eindhoven, The Netherlands), operating at an accelerating voltage of 200 KeV in a bright-field image mode. One drop of the sample dispersion in water (~3 μL, 0.035 mg/mL) was deposited on a carbon film supported on a copper grid (300 mesh), hydrophilized by a glow discharge process just prior to use. After staining for 20 seconds with a uranyl acetate aqueous solution (1% w/v), the sample was rotated at high speed in order to dry at room temperature quickly by spinning process. Number-average diameter was calculated by ImageJ platform analysis using a Gaussian curve fitting after counting about 300 nanoparticles.

Nuclear magnetic resonance (1H NMR and DOSY NMR): NMR spectra were recorded on a Bruker AVANCE III spectrometer at 500 MHz and 25 ºC. Chemical shifts (δ) are given in ppm relative to the residual signal of the solvent. Splitting patterns: b, broad; s, singlet; d, doublet; t, triplet; q, quartet; m, multiplet.

Diffusion Coefficient calculations: Taylor dispersion analysis (TDA) studies were performed on a Viscosizer-TD using fused silica capillaries (40 ºC, 500 mbar). The mobile phase was water and the solutes were monitored by UV absorbance (UV wavelength filter 254 nm) at two fixed windows.

Synthesis of the dextran methacrylated precursor polymer [DXT-MA (DS ~52%)] Dextran methacrylated polymer (**DXT-MA**) was synthesized following a slightly modified published procedure [1S]. Dextran (DXT-40, 1g) was dissolved in 30 mL of dimethyl sulfoxide (DMSO) under a nitrogen atmosphere, to this solution 200 mg of 4-(N,N-dimethylamino)pyridine (DMAP, 1.6 mmol) was added. Then, 1 mL of glycidyl methacrylate (GMA, 1.2 mmol) was incorporated and the mixture was stirred at room temperature during 4 days. The reaction was stopped by adding an equimolar amount of concentrated HCl solution (37% v/v, 1.6 mmol, 0.132 mL) to neutralize DMAP. The modified dextran solution was purified by dialysis against distilled water (MWCO 3500 Da) at room temperature until reaching deionized water conductivity values < 1μS (9 days, refreshing with 4 L of deionized water twice per

1S van Dijk-Wolthuis, W. N. E.; Kettenes-van den Bosch, J. J.; van der Kerk-van Hoof, A.; Hennink, W. E. *Macromolecules* **1997**, *30*, 3411−3413.

day). Yield: 75%, DS 52%.1H NMR (500 MHz, D2O) δ ppm: 6.35-6.10 (m, 1H, methacrylic-CH), 5.92-5.72 (m, 1H, methacrylic-CH), 5.54-4.86 (2.4H, including H-1 and H-2/3 MA-substituted), 4.20-3.33 (10.6H, m, rest of Glc), 1.98 (s, 3H, methacrylic-CH3).

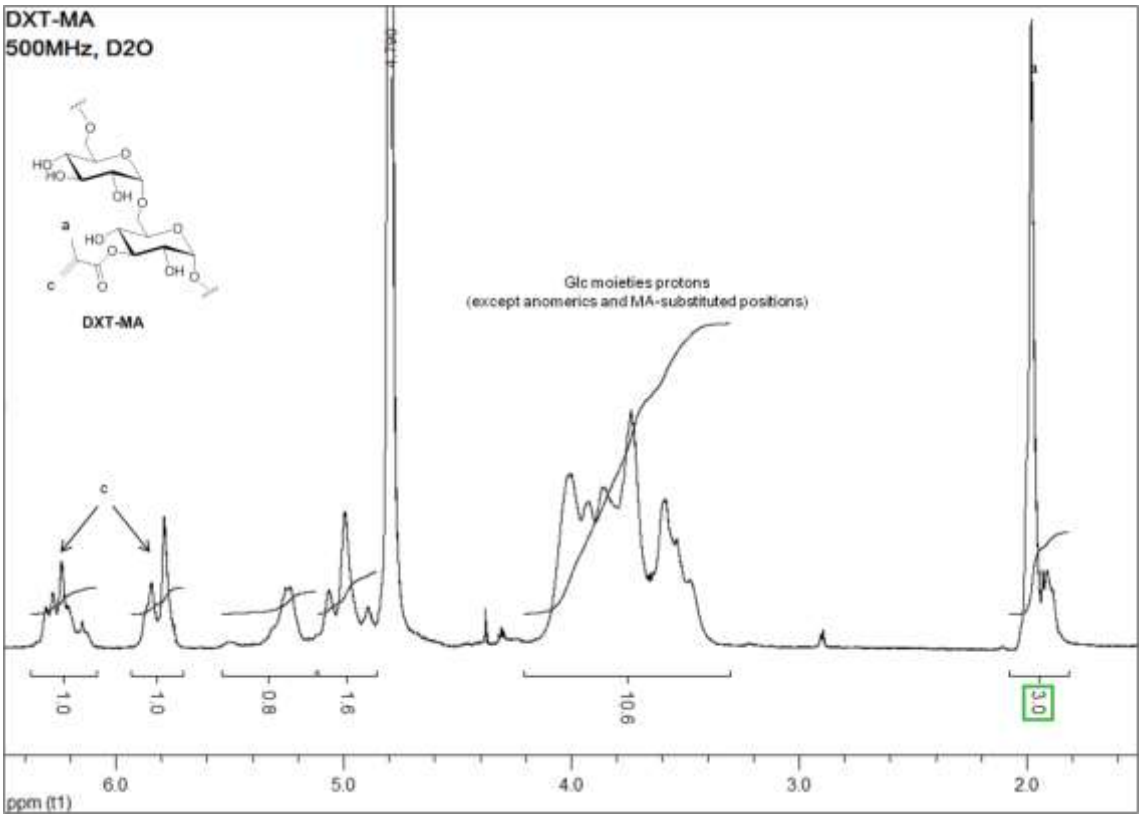

Figure S1: ^{1}H NMR (D_2O, 500 MHz) of **DXT-MA**. For clarity reasons, only MA substitution at position 3 of glucose (Glc) has been depicted. DXT has been drawn as linear polysaccharide (α-1,6 glucosidic linkages) although it is known to be branched, as ramifications (α-1,3 glucosidic linkages) are also present.

The degree of substitution (DS, percent of modified hydroxyl groups per repeating unit) was calculated by 1H NMR through integration of the MA proton signal (integration reference 1.0) with respect to the signals at 3.3-4.2 ppm corresponding to the protons of the glucose (Glc) moiety (6H for unsubstituted Glc and 5H for substituted Glc) except the anomeric protons and the substituted positions (mainly position 3).

Preparation of dextran-based single-chain polymer nanoparticles (DXT-SCPN) In a standard procedure, 0.37 mL of a previously prepared 0.15 M solution (2 mL, MeOH/PBS, 1:1, v/v, pH= 9.5) of cross-linker **DODT** (0.06 mmol, 49 □L) was added dropwise using a syringe pump (0.04 mL/h) over a 0.02 M solution of **DXT-MA** (DS=52%) (100 mg, 0.024 mmol, 13 mL PBS, pH= 9.5) during 8 h at room temperature and under constant stirring. After addition, the reaction was maintained stirred at room temperature for 12 h. Then, the disappearance of the -SH groups from the homobifunctional cross-linker **DODT** was checked by Ellamn´s test. Further characterization studies were carried out after purification of 5 mL sample from the reaction mixture by dialysis against distilled water (MWCO 3500 Da) until reaching deionized water conductivity values < 1□S (5 days, refreshing with 4 L of deionized water twice per day). Finally the resulting aqueous solution was freeze-dried to obtain nanoparticles as a white solid. Yield >90%. 1H NMR (500 MHz, D2O) δ ppm: 6.34-6.12 (m, 1H, methacrylic-CH), 5.94-5.70 (m, 1H, methacrylic-CH), 5.55-4.85 (5.5H, including H-1 and H-2/3 MA-substituted), 4.34-3.28 (28H, m, rest of Glc and 2xCH2O of cross-linker), 3.06-2.53 (5H, m, C*H*(CH3)C*H2*S, CH2S of cross-linker), 1.98 (s, 3H, methacrylic-CH3), 1.29 (s, 3H, cross-linker-CH3).*Dh* (DLS) = 13 ± 8 nm; PDI 0.2.

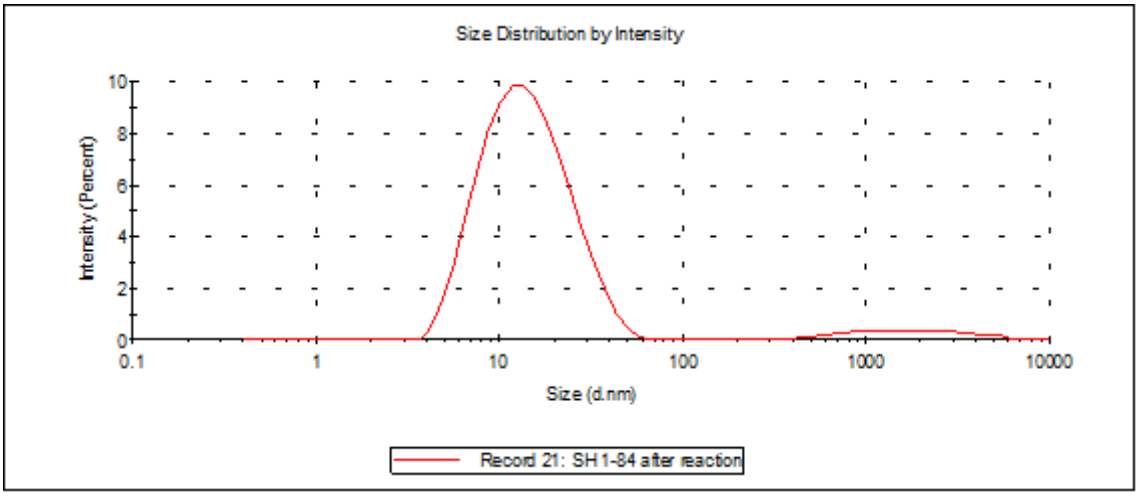

Figure S2: DLS (PBS 10 mM, pH 7.4, 25 ºC) of **DXT-SCPN**.

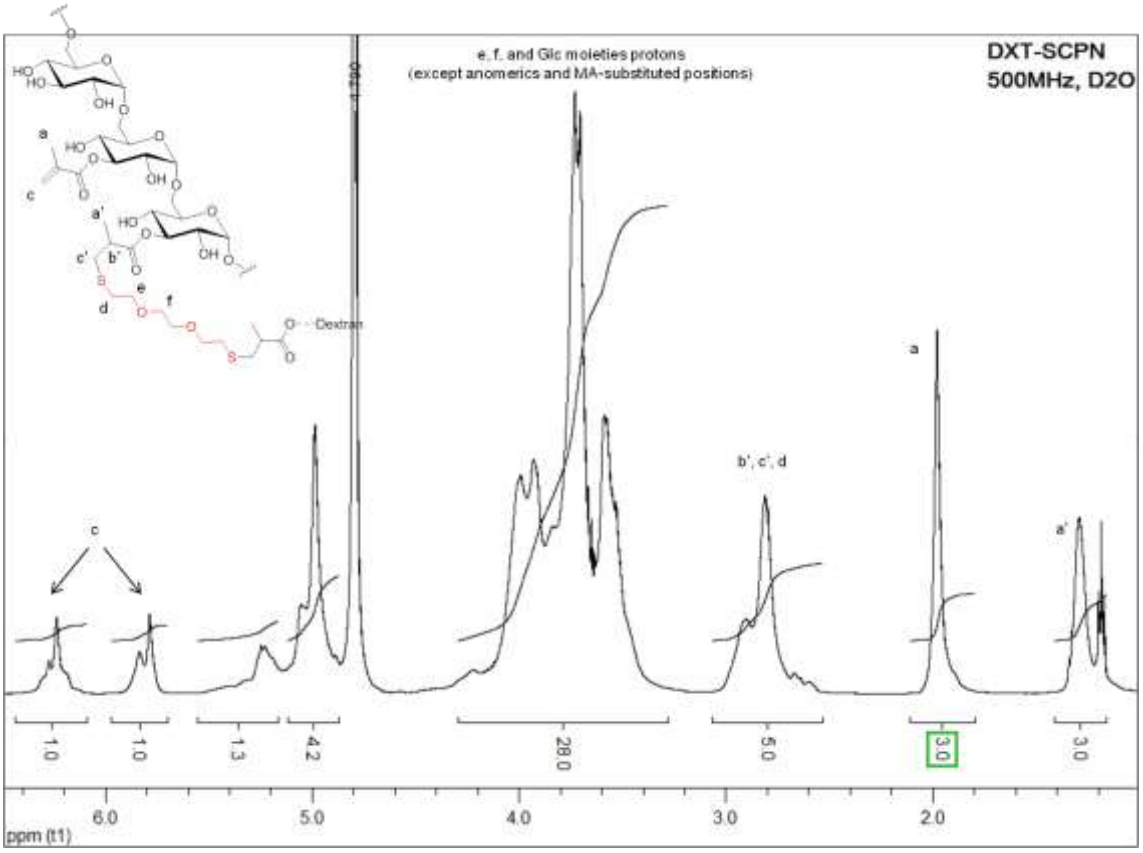

Figure S3: ^{1}H NMR (D_2O, 500 MHz) of **DXT-SCPN**.

Functionalization of DXT-SCPN with 3-mercaptopropionic acid (DXT-SCPN-F)

One batch synthesis of the functionalized **DXT-SCPN-F** was achieved by adding slowly 2 mL of an aqueous solution of 3-mercapto propionic acid (61.4 □L, 7.5 □mol, pH= 9.5) to the reaction flask in the previously reported synthesis of the **DXT-SCPN**. The reaction was stirred for 24 h and the excess acid was removed by dialysis against distilled water (MWCO 3500Da) until reaching deionized water conductivity values < 1□S (5 days, refreshing with 4L of deionized water twice per day). The resulting aqueous solution was freeze-dried to obtain nanoparticles as a white solid. Yield >90%. 1H NMR (500 MHz, D2O) δ ppm: 5.45-4.90 (6H, including H-1 and H-2/3 MAsubstituted), 4.13-3.41 (31H, m, rest of Glc and 2xCH2O of cross-linker), 3.02-2.71(8H, m, 2x C*H*(CH3)C*H2*S, CH2S of cross-linker and MPA), 2.70-2.49 (2H, m, C*H2*COOH of MPA), 1.29 (s, 5.4H, cross-linker- and MPA-CH3) *Mw* (GPC) =

38KDa,*Mw*/*Mn* = 1.7; *Dh* (DLS) = 15 ± 4 nm; PDI 0.2, Zetapotential (pH = 7.2, 25 °C) = -20mV ±5. TEM (uranyl acetate staining): 13 ± 3 nm.

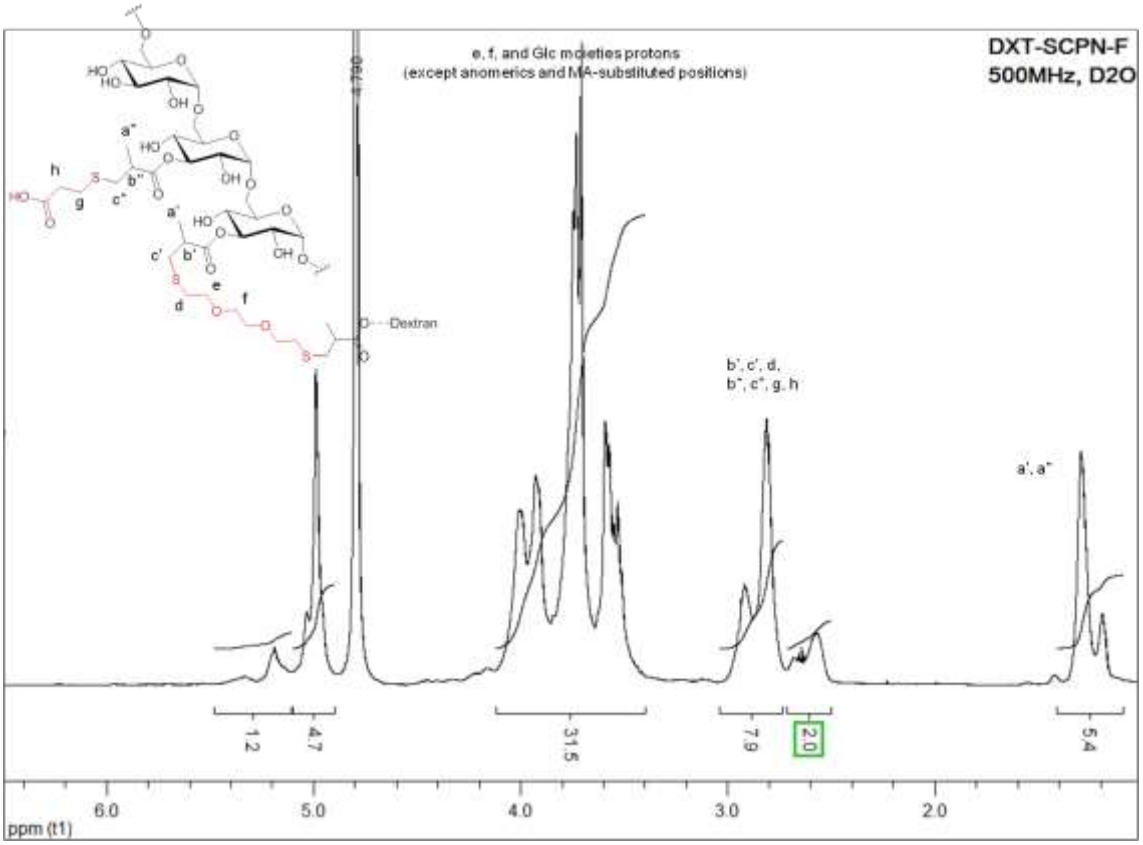

Figure S4: ^{1}H NMR (D_2O, 500 MHz) of SCPNs functionalized with MPA (**DXT- SCPN-F**).

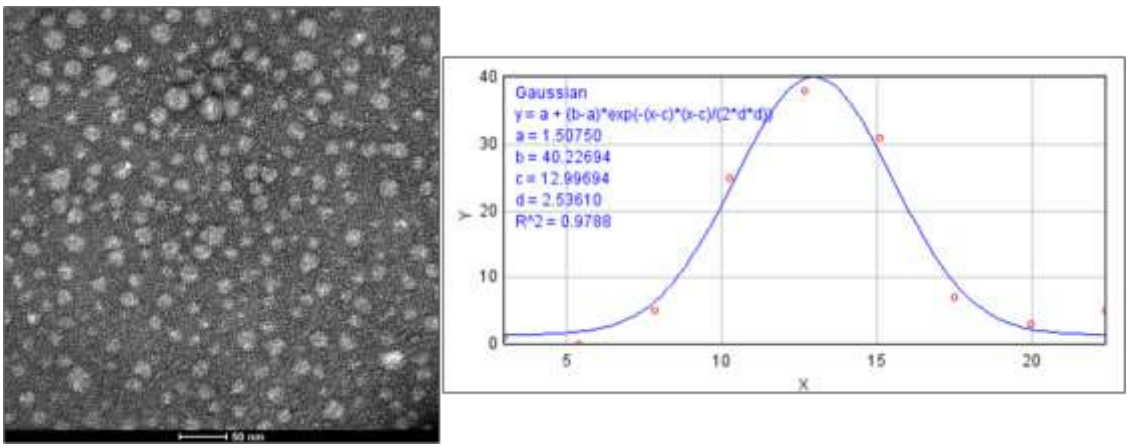

Figure S5: TEM (uranyl staining) and distribution analysis (number-average diameter calculated by ImageJ platform using a Gaussian curve fitting after counting about 300 nanoparticles) of **DXT-SCPN-F**.

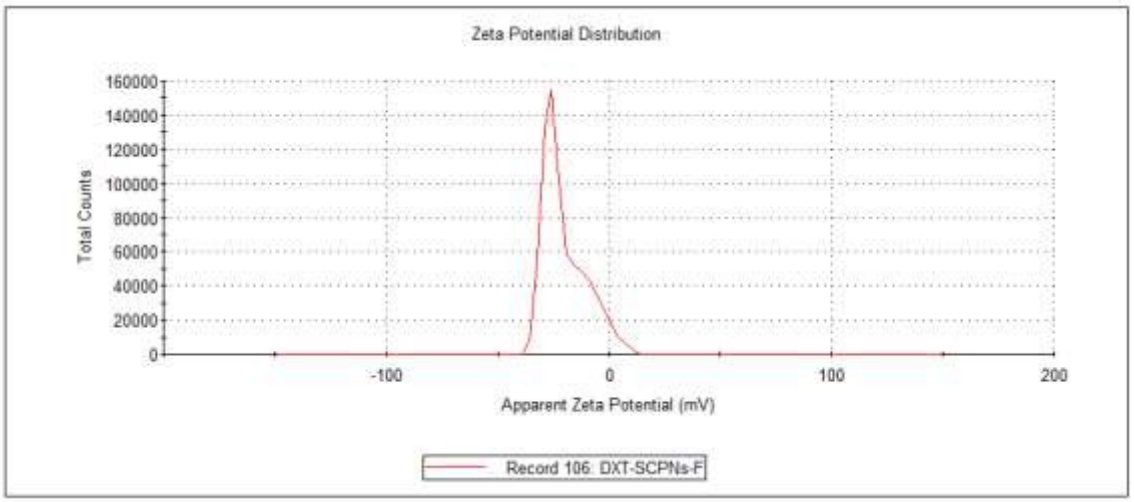

Figure S6: Z-potential measurement (1mM NaCl) of **DXT-SCPN-F** (pH = 7.2, 25 °C).

Functionalization of the DXT-MA (52%) with 3-mercaptopropionic acid (DXTMA-F)

An aqueous solution of 3-mercaptopropionic acid (430 □L, 5 mL H2O, pH= 9.5) was slowly added to a previously prepared solution of **DXT-MA** (DS 52%) (350 mg, 20 mL H2O, pH= 9.5). The reaction was maintained under constant stirring for 12 h and then purified by dialysis against distilled water (MWCO 3500Da). The resulting aqueous solution was freeze-dried to obtain the resulting quenched polymer as a whitesolid. *Mw* (GPC) = 47 KDa, *Mw*/*Mn* = 1.7. Zetapotential (pH = 7.2) = -12 mV ± 7.

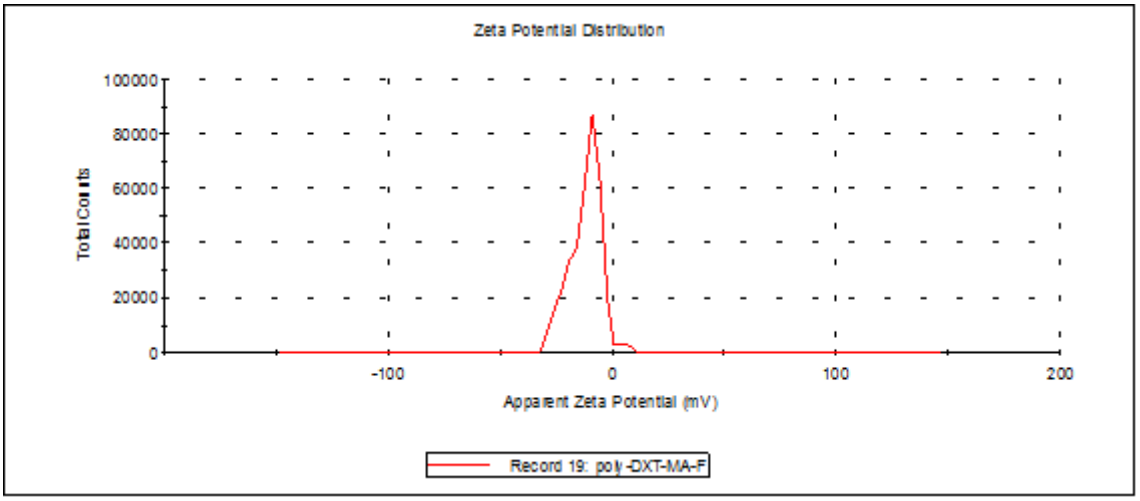

Figure S7: Zeta potential measurement (1 mM NaCl) for **DXT-MA-F** (pH = 7.2, 25 °C).

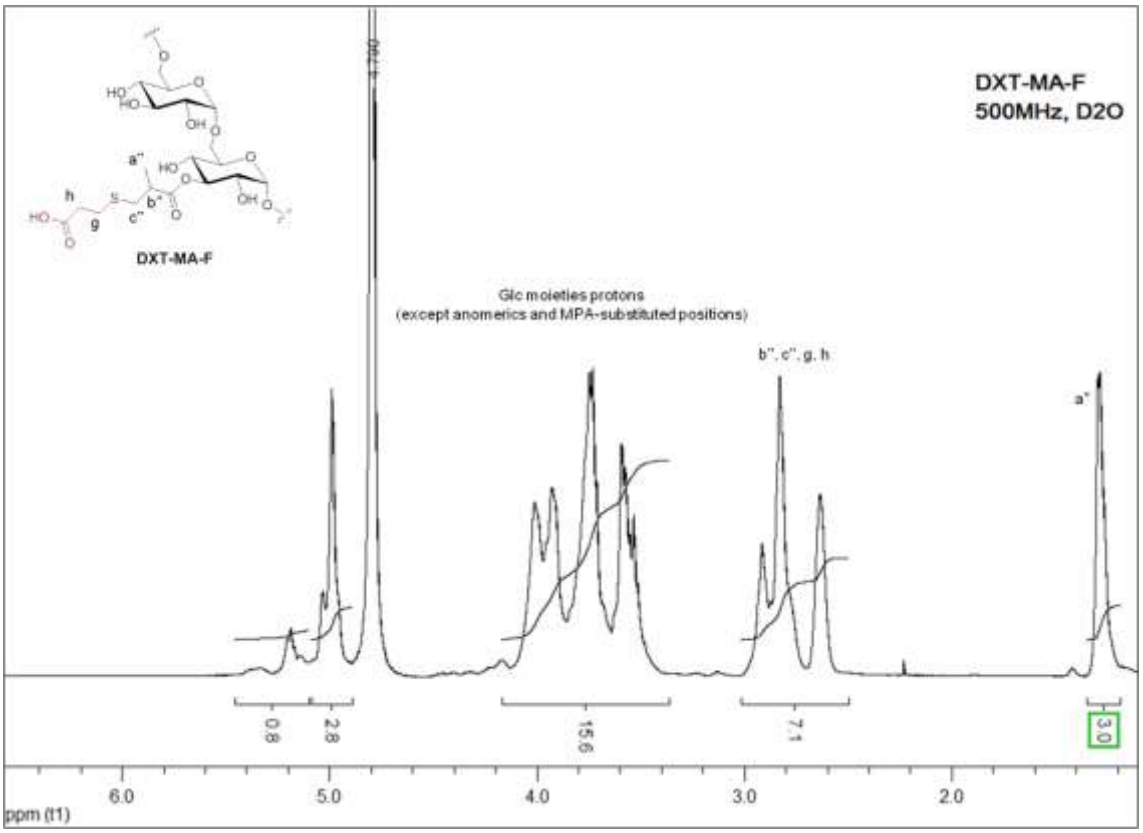

Figure S8: ^{1}H NMR (D_2O, 500 MHz) of **DXT-MA** functionalized with mercaptopropionic acid **(DXT-MA-F)**.

Cytotoxicity

In vitro cytotoxicity studies were carried out with the MTS assay, after 48 h of exposure to increasing concentrations of nanoparticle ranging from 6.25 to 50 μg/mL.

Cell viability analysis showed that under the conditions of this study none of the tested concentrations caused a significant decrease in cell viability when compared with none treated cells (Figure S7). Moreover, morphological analysis of Hela cells showed a typical epithelial adherent morphology.

Cell culture: HeLa cells were cultured in medium containing EMEM (Gibco), 10% fetal bovine serum (Lonza), 1X non-essential amino acid (NEAA) (Sigma), 1% penicillin/ streptomycin (Sigma), 2 mM L glutamine (Sigma). Trypsin (0.25%)/EDTA were used to harvest the cells at 80% confluence. Cell cultures were maintained at 37 ºC in an incubator with 95% humidity and 5% of CO2. The cultures were replenished with fresh medium at 37 ºC twice a week.

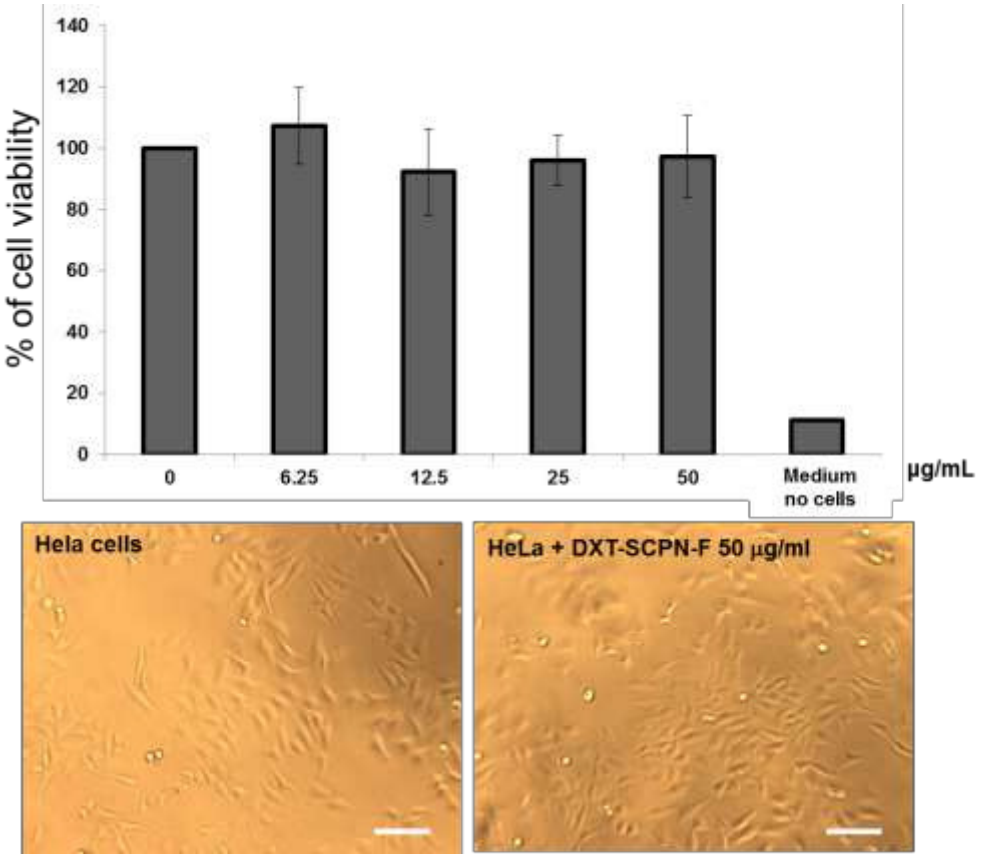

Figure S9: Cytotoxicity studies. MTS cell viability assay of HeLa cell exposed to increasing concentrations of dextran-based single-chain nanoparticles (**DXT-SCPN-F**) ranging from 6.25 to 50 g/mL. Scale bar 200 µm.

MTS assay: HeLa cell growth was evaluated using Cell Titer 96 ® Aqueous One Solution Cell proliferation Assay (Promega). HeLa cells were seeded at a density of 10000cl/cm2 in p96 well plates and allowed to grow for 24 h. After removing the medium, 100 µl of HeLa medium containing various concentrations nanoparticles ranging from 6.25 to 50 µg/mL were added and further incubated for 48 h. At 48 h post nanoparticles incubation, cells were cultured in a 37 ºC of humidified incubator for 2 h with 20µL of Cell Titer 96 ® Aqueous One Solution Reagent containing tetrazolium compound [3-(4,5-dimethylthiazol-2-yl)-5-(3-carboxymethoxyphenyl)-2-(4 sulfophenyl)-2H-tetrazolium)] and an electron coupling reagent, phenazine ethosulfate (PES) per 100 µL of cultured media. The absorbance per well was measured at 490 nm using a micro-plate reader (Multiscan ascent, Thermo). All experiments were performed in triplicate.

Functionalization of the SCPNs with NODA and radiolabeling for *in vivo* biodistribution studies

Functionalization: To a stirred solution of **DXT-SCPN-F** (20 mg) in DMSO (8 mL), 10mg of DMTMM·HCl (0.04 mmol) were added and the mixture was maintained under constant stirring for 15 min. Then, a solution of **NH2-NODA-GA** (10mg, 0.02mmol) in DMSO (1mL) was added to the reaction flask and the reaction was stirred at room temperature for 12 h. The reaction was purified by dialysis against distilled water(MWCO 1000 Da) until reaching deionized water conductivity values (< 1 □S). Theamount of NODA (0.1mg NODA/1mg **DXT-SCPN-F**) was calculated by loading Zn(II)which concentration was determined by colorimetric titration in acetate buffer (pH=4.5)using xylenol orange as the indicator. *Dh* (DLS) = 14 ± 9 nm; PDI 0.2, Zetapotential (pH=7.2) = -12 mV ± 7.

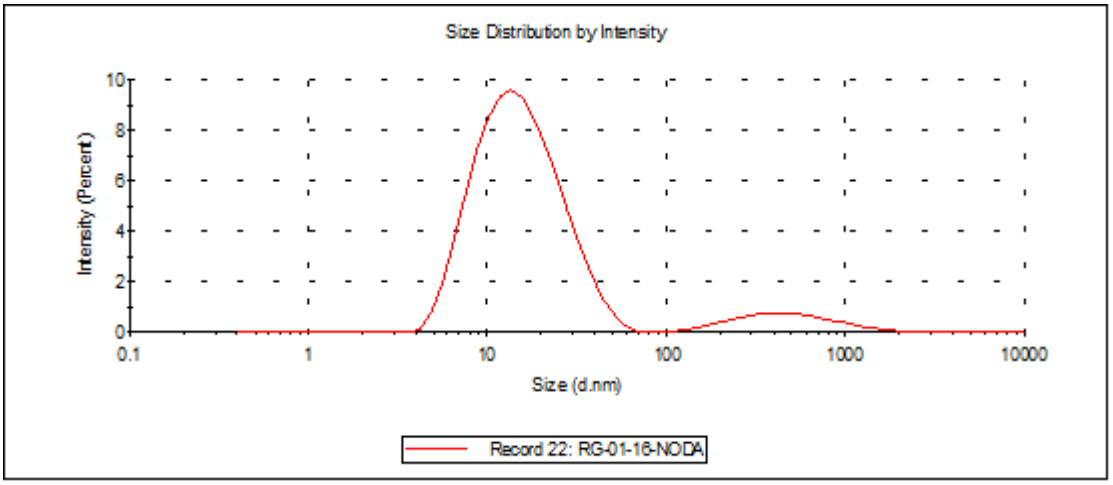

Figure S10: DLS (PBS 10 mM, pH 7.4, 25 ºC) of **DXT-SCPN-NODA**.

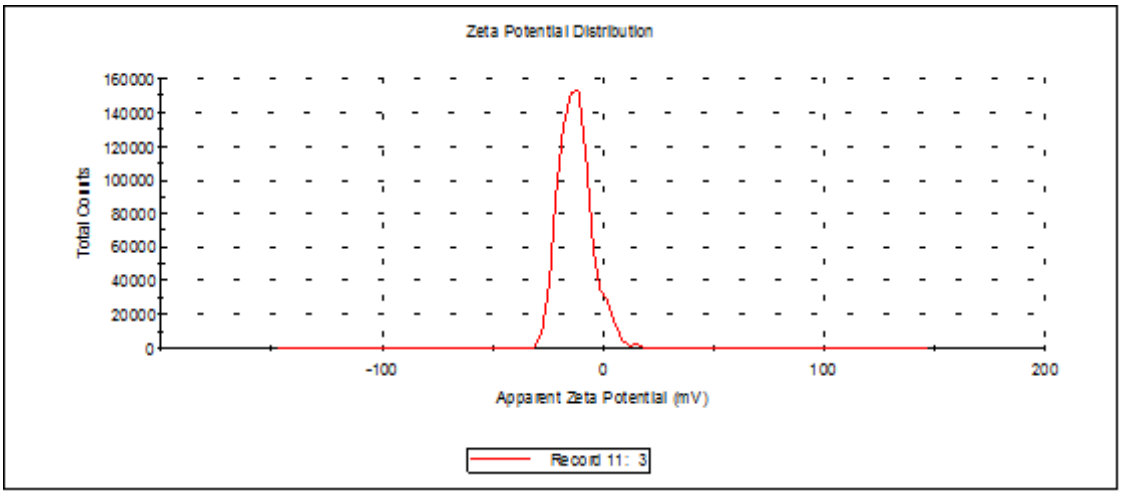

Figure S11: Zeta potential measurement (1mM NaCl) for NODA-functionalized SCPNs (**DXT-SCPN-NODA**) (pH = 7.2, 25°C

Radiolabelling of SCPNs: Gallium-67 (^{67}Ga) was obtained from Mallinckrodt Medical, B.V. (Le Petten, The Nederlands) as citrate salt. Prior to radiolabelling reactions, ^{67}Ga citrate was converted into ^{67}Ga chloride using a previously described method, with minor modifications [2S]. In brief, the ^{67}Ga citrate solution was first eluted through two silica cartridges connected in series (Sep-Pak® Silica Plus Light, Waters Co., Milford, MA, USA) at a constant flow rate of 0.1 mL/min. The cartridges were dried with air for 1 minute and washed with ultrapure water (5 mL, obtained from a Milli-Q® Purification System, Millipore®, Merck KGaA, Darmstadt, Germany). Desorption of ^{67}Ga ions was finally achieved by elution with 0.1 M aqueous HCl solution (1 mL) at a flow rate of 0.1 mL/min. The eluate was collected in different fractions (ca. 100 µL each) and those fractions containing the maximum activity concentration (typically fractions 4-5) were used in subsequent labelling experiments.
Radiolabeling of SCPNs was performed by incubation of the NODA-functionalized nanoparticles (**DXT-SCPN-NODA**) with ^{67}GaCl3. In a typical experiment, 50 µL of SCPNs solution (1 mg/mL) and 50 µL of ^{67}GaCl3 were incubated in sodium acetate buffer solution (0.2M, pH = 4.2, 200 µL). The mixture was incubated at 25°C for 45 min. After incubation, the crude material was purified by centrifugal filtration using Millipore Amicon® Ultra filters (3 kDa cut-off). The resulting precipitate was washed three times with sodium acetate buffered solution to remove unreacted ^{67}Ga species, and the amount of radioactivity in the pellet, the supernatant and the washings were determined in a dose calibrator (CPCRC-25R, Capintec Inc., NJ, USA). Labelling efficiency (expressed in percentage) was calculated as the ratio between the amount of radioactivity in the filter and the total amount of radioactivity in all fractions. Finally, the nanoparticles were suspended in 0.2 M sodium acetate buffer solution (pH 4.2). Radiochemical yield was calculated as the ratio between the amount of radioactivity in the resuspended fraction and the starting amount of radioactivity.

Radiochemical stability of SCPNs: Radiolabelled nanoparticles prepared as described above were incubated in sodium acetate buffered solution at 37 °C using a digital block heater. At different time points (1, 3, 24, 48, 72 and 144 h) samples were withdrawn and the amount of radioactivity was measured. The 67Ga-radiolabelled SCPNs were filtered, washed twice with ultrapure water, and the amount of radioactivity in the filter and the filtrate/washings was measured. The radiochemical stability was calculated as the percentage of radioactivity in the pellet with respect to the total amount of radioactivity (pellet + filtrate + washings).

Animal studies: Animals were maintained and handled in accordance with the Guidelines for Accommodation and Care of Animals (European Convention for the Protection of Vertebrate Animals Used for Experimental and Other Scientific Purposes). All animal procedures were performed in accordance with the Spanish policy for animal protection (RD53/2013), which meets the requirements of the European Union directive 2010/63/UE regarding their protection during experimental procedures. Experimental procedures were approved by the Ethical Committee of CIC biomaGUNE and authorized by the regional government

Administration of the radiolabelled SCPNs: Six-to–eight weeks-old female Sprague Dawley rats (Janvier, Le Genest-Saint-Isle, France) were used. Rats were anesthetized by an intraperitoneal injection of a mixture of medetomidine, midazolam and fentanyl (0.6, 6 and 0.02 mg/Kg, respectively). Once animals (n = 4) were under sedation, 67Garadiolabelled SCPNs were administered by intratracheal nebulization using a Penn- Century MicroSprayer® Aerosolizer (FMJ-250 High Pressure Syringe Model, Penn- Century. Inc. Wyndmoor, USA). A small animal Laryngoscope (Model LS-2, Penn- Century. Inc.) was used for correct visualization of the epiglottis, ensuring a correct positioning of the tip just above the carina. A pre-defined volume of radiolabelled SCPNs (50 µL, established by using spacers in the syringe plunger) was administered (amount of radioactivity around 1.85 MBq). Immediately after, rats were submitted to *in*
vivo imaging studies.

In vivo imaging studies: Immediately after administration of the radiolabeled SCPNs, and without recovering from sedation, animals were positioned in an eXplore speCZT CT preclinical imaging system (GE Healthcare, USA) to perform *in vivo* studies. Body temperature was maintained with a homeothermic blanket control unit (Bruker BioSpin GmbH, Karlsruhe, Germany) to prevent hypothermia, and SPECT scans were acquired for 30 min. After the SPECT scan, a CT acquisition was performed to provide anatomical information of each animal. The SPECT images were reconstructed using a
ordered-subset expectation maximization (OSEM) iterative algorithm (3 iterations/3 subsets, 128 x 128 x 32 array with a voxel size of 0.55 x 0.55 x 2.46 mm3), whereas for the CT a cone beam filtered back-projection a Feldkamp

algorithm (437 x 437 x 800 array with a voxel size of 0.2 x 0.2 x 0.2 mm3) was used. After reconstruction, images were quantified using πMOD analysis software (version 3.4, PMOD Technologies Ltd.). Volumes of interest (VOIs) were manually drawn in the lungs on the CT images and translated to the SPECT images. The relative concentration of radioactivity in the different VOIs was finally determined.